Characterization and Properties of Cellulose Nanofiber/ Polyaniline Film Composites Synthesized through *in Situ* Polymerization

Wen He,[a] Jiaxi Tian,[b] Jiping Li,[b] Hui Jin,[b] and Yanjun Li [a,*]

Cellulose nanofiber/polyaniline (CNF/PANI) composites films were synthesized through *in situ* polymerization of aniline in a nanocellulose suspension that was isolated from bamboo (*Phyllostachys nidularia* Munro). The PANI contents were 5 wt.%, 15 wt.%, or 30 wt.%. Scanning electron microscopy (SEM) and transmission electron microscopy (TEM) showed that the CNF nanofibril surfaces were uniformly coated by PANI particles. Moreover, Fourier transform infrared (FTIR) spectroscopy analysis indicated the formation of hydrogen bonds between the amine groups of aniline and the hydroxyl groups of cellulose. X-ray diffraction (XRD) analysis demonstrated that the cellulose I structure of CNF in the composites did not change, while the crystallinity of CNF was affected. Thermogravimetric analysis (TGA) showed that the thermal stability of CNF was increased due to the addition of PANI. Meanwhile, the obtained electrical conductivity and mechanical properties of the CNF/PANI composites indicated that the composites could be used potentially in anti-static materials, for shielding of electromagnetic radiation, and in biological sensors.

Keywords: Phyllostachys nidularia Munro; Cellulose nanofibers; Polyaniline; Thermal stability; Electrical conductivity; Mechanical properties

Contact information: a: College of Materials Science and Engineering; b: College of Biology and the Environment, Nanjing Forestry University, Nanjing 210037, China;
** Corresponding author: 332812331@qq.com*

INTRODUCTION

Cellulose nanofibers (CNF) have a high aspect ratio with typical lateral dimensions of 5 to 20 nm and longitudinal dimensions ranging from tens of nm to several microns (Vandenberg *et al*. 2007). Materials made from CNF have superior properties such as little thermal expansion, outstanding mechanical properties, sustainability, biocompatibility, and assembly capacity. They have been widely studied relative to their use as reinforcing agents in composite materials, substrates for electronic displays or electrical condensers, oxygen-barrier layers in food packaging, and functional aerogels (Marcovich *et al*. 2006; Vandenberg *et al*. 2007; Meng *et al*. 2009; Casado *et al*. 2012). Moreover, the large number of hydroxyl groups on the surface of CNF creates high chemical reactivity, which further expands the applications of nano-structure cellulose materials (Klemm *et al*. 2005).

Polyaniline (PANI) has been extensively studied as a conducting polymer because of its low cost, ease of preparation, environmental stability, and tunable characteristics (Rudge *et al*. 1994; Dalmolin *et al*. 2009; Patil *et al*. 2012). In general, the applications of PANI are focused on supercapacitors, novel optoelectronic devices, biological sensors, actuators, and electromagnetic shielding (Sainz *et al*. 2005; Casado *et al*. 2012; Zhang *et al*. 2012). However, its difficulty in processing, poor mechanical strength of films, and low

solubility in most of the available solvents constrains the commercial applications of PANI, especially in electromagnetic shielding or flexible optoelectronic devices. To solve these problems, various polymeric materials with good physical properties, such as polystyrene, polyamide, and polysaccharide, have been combined with PANI to obtain good composites (Barthet *et al*. 1998; Fatyeyeva *et al*. 2011). Poly(vinyl alcohol) (PVA) and poly(N-vinylpyrrolidone) have also been reported to improve the processability of PANI as steric stabilizers in PANI dispersions (Stejskal *et al*. 1996).

Many cellulose-based materials, including cellulose acetate, bacterial cellulose hydrogel, bacterial cellulose membrane, and cotton linter pulp have been used to fabricate cellulose/PANI composites by different processing approaches (Hu *et al*. 2011; Qaiser *et al*. 2011; Shi *et al*. 2011, 2012). The mechanical properties and processability of PANI composites are significantly improved by the incorporation of different cellulose materials, which can self-assemble into 2-D or 3-D super strong architectures through hydrogen bonding (Razak *et al*. 2013, 2014). Thus, cellulose-based materials show great potential in applications of PANI composites.

The fabrication of CNF/PANI composites has been reported by Luong *et al.* (2013) and Casado *et al*. (2012). The former mainly focuses on the processability of the CNF/PANI composite, while the latter emphasizes sonochemical processing and the thermal properties. In this paper, CNF was isolated from sustainable and environmentally friendly bamboo by a combination of acid treatment and ultrasonication (da Costa Correia *et al*. 2016). To fabricate CNF/PANI composites, the CNF suspension was employed as a platform and stabilizer for the deposition of PANI through *in situ* polymerization. The electrical conductivity, thermal stability, mechanical properties, and morphological features of the CNF/PANI composites were investigated. In addition, interfacial bonding between CNF fibrils and PANI particles and the effect of the PANI coating on the crystallinity of CNF in the composites were examined.

EXPERIMENTAL

Materials

Aniline (99.8%, Acros Organics) and ammonium persulfate (APS) were purchased from Shanghai Innochem Science and Technology Co. (Shanghai, China). Aniline was distilled under reduced pressure in advance. All other chemicals were guaranteed reagents and used without further purification. Distilled water was used in all experiments.

Methods

Extraction of CNF

Phyllostachys nidularia Munro was collected from Yibing County in Sichuan province, China. Bamboo green and tabasheer were removed, and the bamboo slats were ground into particles of 80- to 100-mesh in size. Next, the bamboo particles were treated with an acidified sodium chlorite solution at 75 °C for 1 h, and the process was repeated six times. The delignified particles were washed with distilled water until the solution reached neutral pH. After these treatments, the dried particles were immersed in a 5 wt.% sodium hydroxide solution for 24 h, followed by vigorous agitation at 80 °C for 2 h to remove hemicelluloses. The obtained α-cellulose was hydrolyzed in 64% H_2SO_4 solution at 40 °C for 30 min with intense agitation, and the hydrolysis reaction was terminated by adding distilled water. The diluted hydrolysis suspension was centrifuged until the pH

reached 4 to 5, and the suspension was dialyzed until it reached neutral pH. Finally, the suspension obtained was treated with an ultrasonicator for 15 min in an ice bath. After ultrasonic processing, the obtained white suspension was freeze-dried and collected for further processing.

Preparation of CNF/PANI composite films

PANI was polymerized with an oxidative synthetic method proposed by Luong *et al*. (2013). First, aniline monomer (ANI) was dispersed in CNF suspension (1 g/L) by ultrasonication treatment according to a set of CNF/ANI ratios of 100/0, 95/5, 85/15, and 70/30 wt./wt.%. APS solution dissolved in aqueous HCl (1 M) was added dropwise to CNF/ANI suspensions at an APS/ANI ratio of 1.25 wt/wt.%, and the mixture was kept in an ice bath with magnetic stirring for 12 h. The green CNF/PANI suspensions were dialyzed in water using a membrane (0.2 μm, pall 60301 Supor, USA), with fresh exchanges of water until it became colorless. The solutions were doped in 1 M HCl to eliminate all impurities. CNF/PANI composites were separated from the HCl by ultra-centrifugation (12 min at 12,000 rpm) and washed with distilled water until CNF/PANI composites reached neutral pH. Finally, CNF/PANI composite films were prepared by casting the washed suspensions on a glass Petri dish and drying for 24 h at 45 °C. As a control, CNF film and PANI particles were prepared with the same procedure.

Measurements

Transmission electron microscopy (TEM)

Dilute suspensions (0.01 mg/mL) of the nanocellulose fibers and the CNF/PANI composite were deposited on a carbon-coated copper grid. The excess suspension was removed by blotting with a filter paper. The sample was stained with a droplet of fresh uranyl acetate (2 wt.%), which was added to the grid. The excess solution was removed by blotting with a filter paper, and the sample was allowed to dry. Samples were visualized with a Hitachi transmission electron microscope (HT-7700, Tokyo, Japan) operated at 80 kV.

Scanning electron microscopy (SEM)

The morphology in horizontal plane and cross section of the CNF/PANI composite films were investigated using a scanning electron microscope (JSM-7600F, JEOL Ltd., Kyoto, Japan) at an acceleration voltage of 15 kV. Specimens were coated with gold for 60 s with a vacuum sputter coater (Quorum Q150TES, London, UK).

Fourier transform infrared (FTIR) spectroscopy

The FTIR spectra of CNF, PANI, and CNF/PANI composites were investigated on a Nicolet Magna 560 spectrometer (Washington D.C., USA). The specimens were blended with KBr powder and compressed to form a disk. The spectra for each specimen were detected in the range from 4000 to 500 cm^{-1} at a resolution of 4 cm^{-1}.

Electrical properties

Electrical conductivity of CNF/PANI composite films containing different PANI contents were measured at room temperature by a four-point probe method using the multi-height probe combined with the RM3000 test unit from Jandel Engineering Ltd. (Suzhou, China). The electrical conductivity of PANI was also measured by pressing the powder at 8 MPa for 5 min using a hydraulic press. The probe was equipped with four tungsten

carbide needles having a diameter of 100 µm and spaced 1 mm apart. Sheet resistance (R_s, ohms per square) and thickness (t, cm) were used to calculate the specific resistivity (ρ, Ω • m) and the corresponding conductivity (σ, S/cm).

$$\rho = R_s \times t \quad (1)$$

$$\sigma = 1/\rho \quad (2)$$

Mechanical properties

The tensile strength, Young's modulus, and strain at break of all specimens were measured using an UH2503 universal testing machine (Superior control technology (Shanghai) Co., Ltd., Shanghai, China) following the ASTM with a test speed of 0.5 mm/min. The testing environment was maintained at 45% relative humidity and 25 °C. The specimen dimensions were 45 mm × 20 µm × 5 mm, and at least six samples were prepared for each specimen.

Thermo gravimetric analysis (TGA)

TGA was carried out on a TGA Q50 (TA Instruments, Washington D.C., USA) following the ASTM D3850-94 standard (2000). Approximately 8 to 10 mg of the specimen was loaded in the open platinum pan. The samples were heated from 30 to 500 °C under nitrogen atmosphere at constant heating rates of 10 °C /min.

X-ray diffraction (XRD)

The X-ray diffraction (XRD) analysis was performed with a D/max 2200 diffractometer (Rigaku, Kyoto, Japan) using Ni-filtered CuKa radiation (k = 1.5406 Å) at 40 kV and 30 mA. Scattered radiation was recorded in the range of 2θ = 5 to 60° at a scan rate of 5°/min.

RESULTS AND DISCUSSION

Morphological Characteristics

Optical photographs of CNF and CNF/PANI composites films are shown in Fig. 1. The CNF film was transparent, and the CNs/PANI composite films gradually turned darker green in color as PANI content was increased, as previously noted (Luong *et al*. 2013).

Figure 2a shows the diameters of CNF dispersed in deionized water, and the average diameter was around 40 nm. The average diameter of CNF/PANI composite fiber was about 120 nm (Fig. 2b). This increase in CNF diameter was due to the successful deposition of PANI particles on the CNF surface. After mixing, the ANI monomer was absorbed on CNF surfaces *via* hydrogen bonding between the amine groups of aniline and the hydroxyl groups of cellulose, which also ensured the uniform distribution of ANI monomers on the CNF surfaces (Casado *et al*. 2012). Subsequently, aniline monomers on the CNF surface were polymerized by APS, resulting in a color change.

Figure 3a shows that pure CNF film presented an intertwined network of high-aspect-ratio nanofibers with diameters of 30 to 40 nm and relatively smooth surfaces. However, the CNF/PANI composite fiber diameters were significantly larger than those of neat CNF film (Fig. 3b, c, and d). Moreover, the diameters of CNF gradually increased with increasing PANI content. This result indicated that CNF fibers were completely

enclosed by the PANI coating, which was comprised of small and uniform particles of several tens of nm in diameter (Meng *et al*. 2009; Mo *et al*. 2009).

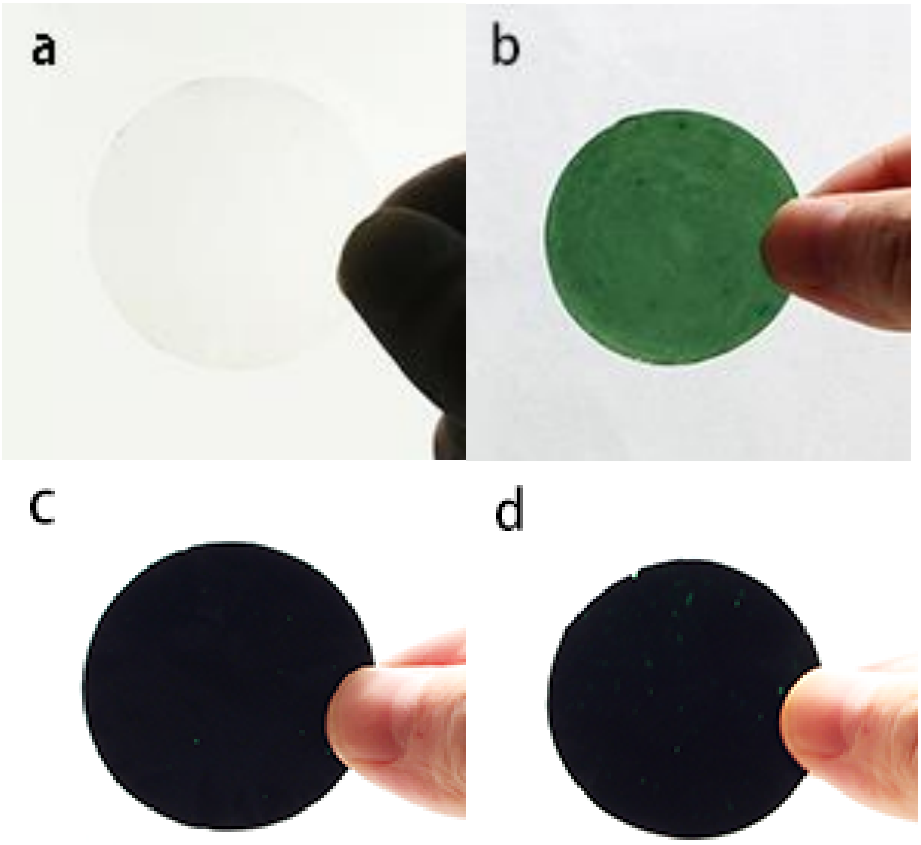

Fig. 1. Photographs of (a) CNF and CNF/PANI composite films containing (b) 5, (c) 15, and (d) 30 wt.% PANI

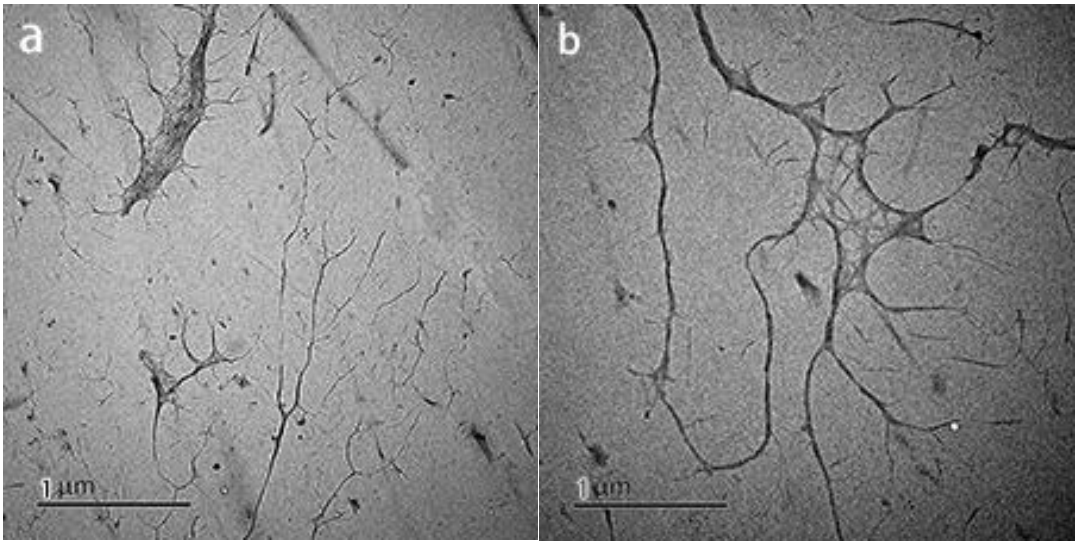

Fig. 2. TEM images of (a) CNF film and (b) the CNF/PANI composite film with 5 wt.% PANI

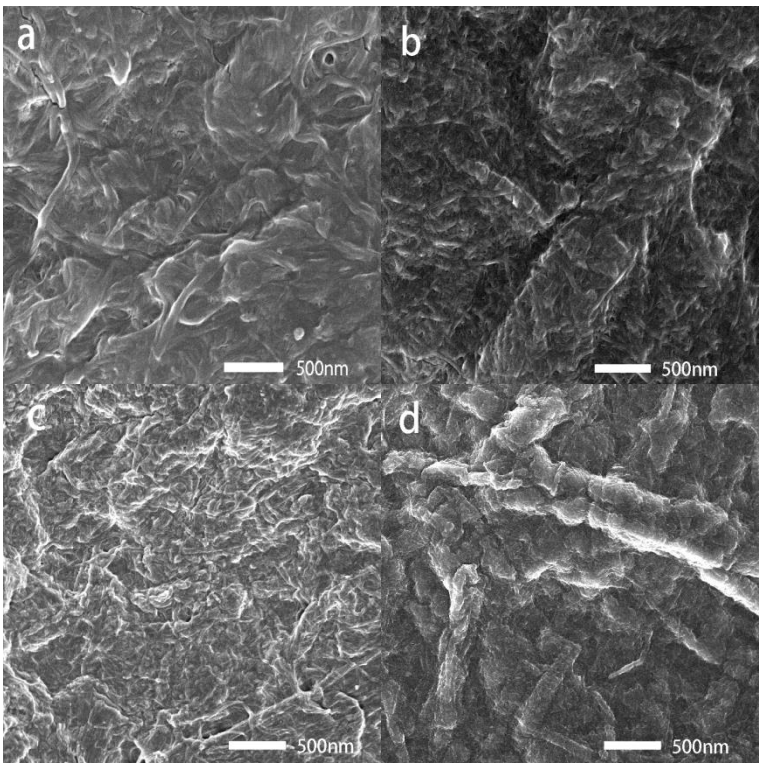

Fig. 3. SEM images of CNF film (a), and CNF/PANI composite films containing different content of PANI from 5 to 30 wt.% (b: 5 %, c: 15 %, and d: 30 %, respectively).

FTIR Analysis

The FTIR spectra of CNF, PANI, and CNF/PANI composites illustrated the morphological characteristics and possible interfacial bonding between CNF and PANI (Fig. 4). The CNF spectrum showed a series of peaks characteristic to cellulose, of which the dominant peaks occurring at 3307 cm^{-1} and 2879 cm^{-1} were attributed to the OH-stretching and CH-stretching, respectively (VandenBerg *et al*. 2007). The peaks from 1528 to 1260 cm^{-1} were associated with the H–O–H stretching vibration of absorbed water in carbohydrates, C–O stretching, and C_1-H deformation vibrations of cellulose, (John *et al*. 2010; Sehaqui *et al*. 2011).

For the FTIR spectrum of PANI, the peak at 797 cm^{-1} was assigned to the N–H wag of the secondary amine. Two sharp peaks at 1115 cm^{-1} and 1296 cm^{-1} in the characteristic spectrum of PANI were attributed to the aromatic amine (Ohira *et al*. 1987). The peaks at 1482 and 1568 cm^{-1} were ascribed to the stretching vibrations of N–B–N and N=Q=N structures, respectively; B and Q are abbreviations of benzenoid and quinoid moieties in the PANI polymers (Rezaei *et al*. 2011; Yu *et al*. 2012). Although the FTIR spectrum of the CNF/PANI composite showed the characteristic peaks of both CNF and PANI, there were some notable changes. Distinctly, all the characteristic peaks of the CNF/PANI composite were shifted to lower frequencies compared with those of pristine PANI, which could be due to the cleavage of hydrogen bonds in PANI particles and pure CNF (Mo *et al*. 2009; Kebiche *et al*. 2012; Lissarrague *et al*. 2012). Moreover, the intensity of the OH peak (around 3265 cm^{-1}) and NH peak (around 792 cm^{-1}) in the CNF/PANI composite was significantly decreased compared with pure CNF and PANI. The change could be ascribed to weakened intermolecular hydrogen bonding in CNF, by which more hydroxyl groups in

CNF are accessible, leading to the uniform coating of PANI in the cellulose nanostructure (Šedeˇnková *et al*. 2008). In sum, the morphological characteristics and FTIR analysis showed that PANI closely enwrapped the CNF nanofibers after *in situ* polymerization.

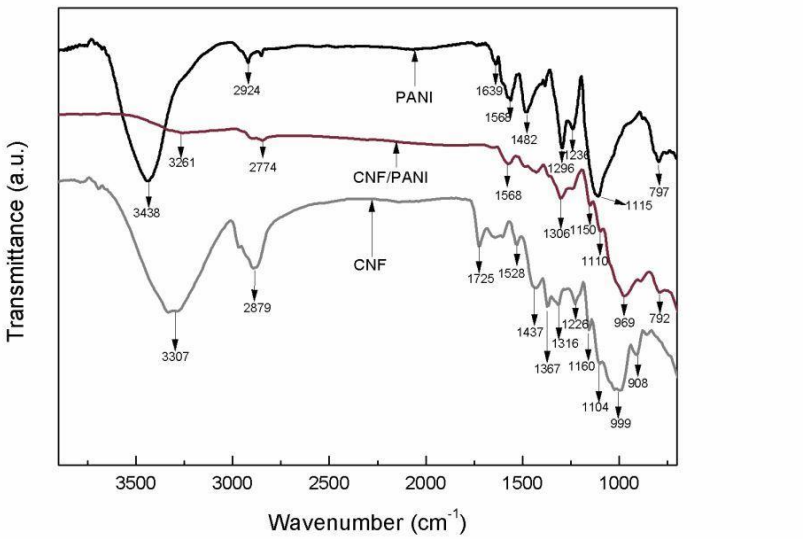

Fig. 4. FTIR spectra of CNF, PANI, and the CNF/PANI composite containing 30 wt.% of PANI

Electrical Properties

Figure 5 shows the electrical conductivities of all CNF/PANI composites. The pure PANI showed a high conductivity value of 1.2 S/cm; however, when the loading content of PANI decreased to 5 wt.%, the composite showed a conductivity value of 8.6×10^{-5} S/cm.

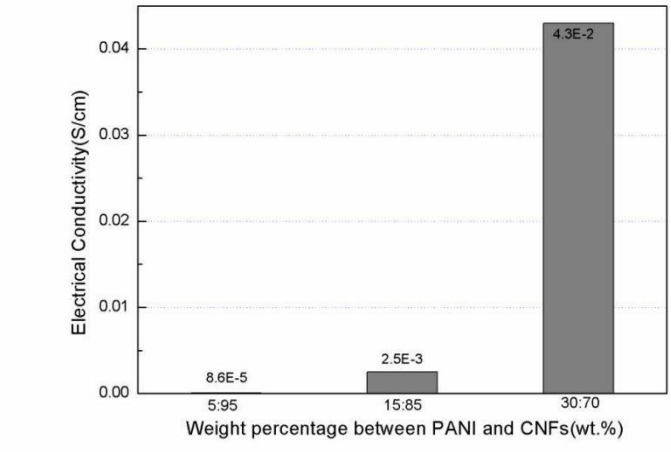

Fig. 5. Electrical conductivity of CNF/PANI composite films with different PANI contents

Although the composite showed lower electrical conductivity, it could be used in applications such as electrostatic dissipation, especially as an antistatic material. In general, the antistatic criterion is in the range of 1×10^{-11} to 1×10^{-9} S/cm, which allows movement

of electrons from higher to lower charge densities and inhibits the delivery of a spark or shock (Ramasubramaniam *et al*. 2003; McLachlan *et al*. 2005).

When the loading content of PANI increased to 30 wt.%, the composite conductivity was significantly enhanced to 4.3×10^{-2} S/cm. Clearly, the electrical conductivity of the composite increased accordingly with increased PANI loading. These conductivity values are suitable for materials that shield electromagnetic radiation (Pääkkö *et al*. 2007).

Table 1. Tensile Properties of Pristine CNF and CNF/PANI Composites

Specimens (Film)	Tensile Strength, σ_b (MPa)	Young's Modulus, E (GPa)	Strain at Break, ε_b (%)
Neat CNF (0%PANI)	132 ± 6	3.8 ± 0.5	8 ± 3
CNF/PANI (95/5 wt.%)	127 ± 5	3.0 ± 0.5	9 ± 4
CNF/PANI (85/15 wt.%)	113 ± 4	2.6 ± 0.3	7 ± 3
CNF/PANI (70/30 wt.%)	98 ± 4	2.1 ± 0.4	7 ± 3

Mechanical Properties

The values of the tensile strength, Young's modulus, and the strain at break are summarized in Table 1. The tensile strength and Young's modulus of pure CNF were about 132 MPa and 3.8 GPa, respectively, while the strain at break was about 8%. The excellent mechanical properties of CNF film are ascribed to the strong intra- and intermolecular hydrogen bonds of the cellulose nanofibrils (Sehaqui *et al*. 2011; He *et al*. 2013). The composite containing 5 wt.% PANI exhibited high mechanical properties, with a mean tensile strength and Young's modulus of 127 MPa and 3.0 MPa, respectively. However, this composite showed a higher strain (approximately 9%) than pure CNF. As the PANI content was increased to 30 wt.%, the mechanical properties of the composite were significantly decreased, with mean values of tensile strength and Young's modulus of 98 MPa and 2.1 GPa, respectively. The decreases in tensile strength and Young's modulus could be ascribed to the weakening of hydrogen bonding in CNF fibrils, which makes hydroxyl groups in CNF accessible to PANI and leads to the uniform coating of PANI in the cellulose nanostructure. However, PANI is a brittle polymer, and increased PANI content led to decreased tensile strength and Young's modulus in CNF/PANI composites (Zhang *et al*. 2012).

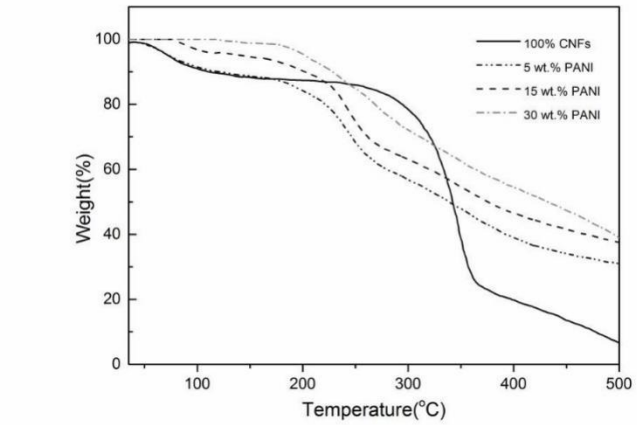

Fig. 6. TGA curves of CNF and CNF/PANI composites containing PANI of 5, 15 and 30 wt.%

Thermogravimetric Analysis

The thermogravimetric curves of pure CNF film and composite films with 5, 15, and 30 wt.% PANI are illustrated in Fig. 6. The slight weight loss of pure CNF film resulted from water evaporation at around 100 °C, and the weight loss centered at about 315 °C was attributed to cellulose pyrolysis (Shi *et al*. 2012). For the composite with 5 wt.% PANI, the light weight loss at around 100 °C was attributed to removal of moisture, and the significant weight loss appeared from 200 to 350 °C may be due to the degradation of HCl dopant and cellulose. Finally, the weight loss at around 400 °C was attributed to the degradation of PANI molecules (Rezaei *et al*. 2011; Lissarrague *et al*. 2012). However, with increased PANI content, the composites with 15 wt.% and 30 wt.% PANI showed higher thermal stability than pure CNFs film, which indicated that PANI acted as a protective barrier against cellulose degradation (Patil *et al*. 2010).

X-ray Diffraction (XRD) Analysis

XRD was used to further characterize the structure of CNF/PANI composites (Fig. 7). Composites containing 15% and 30% PANI were selected for analysis, and pure CNF and PANI were characterized as references. Two peaks at 2θ =15.24° (*110*) and 22.4° (*200*) were observed for CNF, which is the classic cellulose I structure (Pääkkö *et al*. 2007). Two peaks located at 2θ = 21.6° and 24.5° also were observed for the neat PANI microstructures.

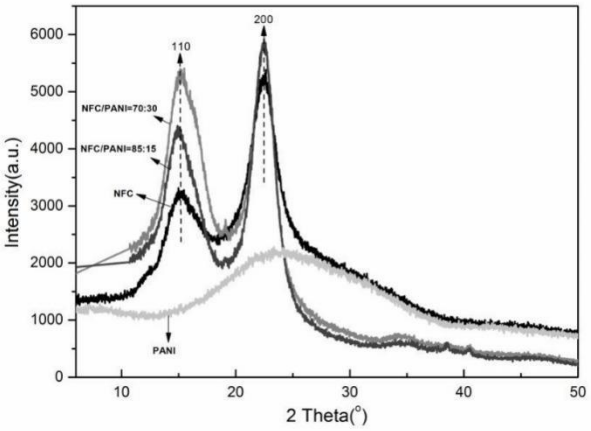

Fig. 7. X-ray diffraction patterns of CNF, PANI, and CNF/PANI composites containing 15 wt.% and 30 wt.% PANI

These peaks were superimposed on broad scatterings centered at 2θ = 15° to 25°, which are ascribed to the periodicity parallel and perpendicular to the polymer chains of PANI, respectively; these characteristics also confirmed that PANI is partially crystalline (Zhang and Wan 2003; Wang *et al*. 2010). Similar to the XRD curve of CNF, two peaks at 15.24° and 22.4° appeared on the diffractive curves of the CNF/PANI composites, indicating that the cellulose I structure of CNF was not destroyed by the *in situ* polymerization of PANI. However, the intensity of peaks at 2θ = 15.24° for CNF/PANI composites was acutely increased. According to the Segal method (Segal and Meshulam 1979), the crystallinity of CNF was decreased due to the formation of hydrogen bonds between hydroxyl groups in the crystalline region of CNF and the amine groups of aniline. Moreover, the crystalline region of CNF was further affected by the increase in PANI, as exhibited by a high intensity peak at 2θ = 15.24° for the composite containing 30% PANI.

CONCLUSIONS

1. A CNF suspension isolated from *Phyllostachys nidularia* Munro was employed as a platform to fabricate CNF/PANI composites through *in situ* polymerization. Based on the morphological characteristics of the composites, the PANI polymer was successfully coated on the surfaces of CNF.
2. The CNF/PANI composites exhibited high electrical conductivity and thermal stability with increased PANI content; however, the mechanical properties gradually decreased with the increase of PANI content, and the NFC/PANI composites showed the worst mechanical characteristics when the PANI content was 30 wt.%.
3. The obtained CNF/PANI composites can potentially be used in many applications such as anti-static materials, electromagnetic radiation shields, biological sensors, and electrically conductive and flexible films.

ACKNOWLEDGMENTS

This study was financially supported by the Natural Science Fund in Jiangsu Province (Grant Number BK20140971), a project funded by the Science and Technology Development of North Area of Jiangsu (Grant Number BN2014069), and the High-level Scientific Research Foundation for the Introduction of Talent in Nanjing Forestry University (GXL2014068). The authors acknowledge financial support provided by the Zhejiang Key Level 1 Discipline of Forestry Engineering (2014lygcy023) and a project funded by the Priority Academic Program Development of Jiangsu Higher Education Institutions (PAPD).

REFERENCES CITED

Barthet, C., Armes, S. P., Chehimi, M. M., Bilem, C., and Omastova, M. (1998). "Surface characterization of polyaniline-coated polystyrene latexes," *Langmuir* 14(18), 5032-5038. DOI: 10.1021/la980102r

Casado, U. M., Quintanilla, R. M., Aranguren, M. I., and Marcovich, N. E. (2012). "Composite films based on shape memory polyurethanes and nanostructured polyaniline or cellulose–polyaniline particles," *Synth. Met.* 162(17-18), 1654-1664. DOI: 10.1016 /j.synthmet.2012.07.020

Dalmolin, C., Biaggio, S. R., Rocha-Filho, R. C., and Bocchi, N. (2009). "Preparation, electrochemical characterization and charge–discharge of reticulated vitreous carbon/polyaniline composite electrodes," *Electrochim. Acta.* 55(1), 227-233. DOI: 10.1016/j.electacta.2009.08.043

Da Costa Correia, V., Maria Siqueira, F., Donizetti Dias, R., and Savastano Junior, H. (2016). "Macro, micro and nano scale bamboo fiber as a potential reinforcement for composites," *Key Engineering Materials*. 46(2), 668-672. DOI: 10.1680/jgrma.15.00026

Fatyeyeva, K., Pud, A. A., Bardeau, J. F., Tabellout, M. (2011). "Structure–property relationship in aliphatic polyamide/polyaniline surface layered composites," *Mater. Chem. Phys.* 130(1), 760-768. DOI: 10.1016/j.matchemphys.2011.07.057

He, W., Jiang, S. X., Zhang, Q. S., and Pan, M. Z. (2013). "Isolation and characterization of cellulose nanofibers from *Bambusa rigida*," *BioResources* 8(4), 5678-5689. DOI: 10.15376/biores.8.4.5678-5689

Hu, W., Chen, S., Yang, Z., Liu, L., and Wang, H. (2011). "Flexible electrically conductive nanocomposite membrane based on bacterial cellulose and polyaniline," *J. Phys. Chem. B* 115(26), 8453-8467. DOI: 10.1021/jp204422v

Kebiche, H., Debarnot, D., Merzouki, A., Poncin-Epaillard, F., and Haddaoui, N. (2012). "Relationship between ammonia sensing properties of polyaniline nanostructures and their deposition and synthesis methods," *Anal. Chim. Acta.* 737(2), 64-71. DOI: 10.1016/j.aca.2012.06.003

Klemm, D., Heublein, B., Fink, H. P., and Bohn, A. (2005). "Cellulose: Fascinating biopolymer and sustainable raw material," *Angew. Chem. Int. Ed.* 36(36), 3358-3363. DOI: 10.1002/anie.200460587

Li, D., Kaner, R.B. (2005). "Processable stabilizer-free polyaniline nanofiber aqueous colloids," *Chem. Commun.* 26(26), 3286-3298. DOI: 10.1039/B504020E

Lissarrague, M. H., Lamanna, M. E., D'Accorso, N. B., and Goyanes, S. (2012). "Effects of different nucleating particles on aniline polymerization," *Synth. Met.* 162(162), 1052-1058. DOI: 10.1016/j.synthmet.2011.12.018

Luong, N. D., Korhonen, J. T., Soininen, A. J., Ruokolainen, J., Johansson, L.-S., and Seppälä, J. (2013). "Processable polyaniline suspensions through in-situ polymerization onto nanocellulose," *European Polymer Journal* 49(2), 335-344. DOI: 10.1016/j.eurpolymj.2012.10.026

Marcovich, N. E., Auad, M. L., Bellesi, N. E., Nutt, S. R., and Aranguren, M. I. (2006). "Cellulose micro/nanocrystals reinforced polyurethane," *J. Mater. Res.* 21(4), 870-881. DOI: http://dx.doi.org/10.1557/jmr.2006.0105

McLachlan, D. S., Chiteme, C., Park, C., Wise, K. E., Lowther, S. E., Lillehei, P. T., Siochi E. J., and Harrison J. S. (2005). "AC and DC percolative conductivity of single wall carbon nanotube polymer composites," *J. Polym. Sci., Part B: Polym. Phys.* 43(22), 3273-87. DOI: 10.1002/polb.20597

Meng, C. Z., Liu, C. H., and Fan, S. S. (2009). "Flexible carbon nanotube/polyaniline paper-like films and their enhanced electrochemical properties," *Electrochem. Commun.*11, 186-189. DOI:10.1016/j.elecom.2008.11.005

Mo, Z. L., Zhao, Z. L., Chen, H., Niu, G. P., and Shi, H. F. (2009). "Heterogeneous preparation of cellulose–polyaniline conductive composites with cellulose activated by acids and its electrical properties," *Carbohydr. Polym.* 75, 660-664. DOI: 10. 1016 /j. carpol. 2008.09.010

Ohira, M., Sakai, T., Takeuchi, M., Kobayashi, Y., and Tsuji, M. (1987). "Raman and infrared spectra of polyaniline," *Synth. Met.* 18(1-3), 347-352. DOI: 10.1016/0379-6779(87)90903-9

Pääkkö, M., Ankerfors, M., Kosonen, H., Nykänen, A., Ahola, S., Österberg, M., *et al.* (2007). "Enzymatic hydrolysis combined with mechanical shearing and high-pressure homogenization for nanoscale cellulose fibrils and strong gels," *Biomacromolecules* 8(6), 1934-1941. DOI: 10.1021/bm061215p

Patil, D. S., Shaikh, J. S., Pawar, S. A., Devan, R. S., Ma, Y. R., Moholkar, A. V., John, A., Mahadeva, S. K., and Kim, J. (2010). "The preparation, characterization and actuation behavior of polyaniline and cellulose blended electro-active paper," *Smart Mater. Struct.* 19(4), 0450-0461. DOI: 10.1088/0964-1726/19/4/045011

Patil, D. S., Shaikh, J. S., Pawar, S. A., Devan, R. S., Ma, Y. R., Moholkar, A. V., Kim, J. H., Kalubarme, R. S., Park, C. J., and Patil, P. S. (2012). "Investigations on silver/polyaniline electrodes for electrochemical supercapacitors," *Physical Chemistry Chemical Physics* 14(34), 11886-11895. DOI: 10.1039/c2cp41757j

Qaiser, A. A., Hyland, M. M., and Patterson, D. A. (2011). "Surface and charge transport characterization of polyaniline-cellulose acetate composite membranes," *J. Phys. Chem. B* 115(7), 1652-1661. DOI: 10.1021/jp109455m@proofing

Ramasubramaniam, R., Chen, J., and Liu, H. (2003). "Homogeneous carbon nanotube/polymer composites for electrical applications," *Appl. Phys. Lett.* 83(14), 2928-2936. DOI: 10.1063/1.1616976

Rezaei, S. J. T., Bide, Y., and Nabid, M. R. (2011). "A new approach for the synthesis of polyaniline microstructures with a unique tetragonal star-like morphology," *Synth. Met.* 161(13-14), 1414-1419. DOI: 10.1016/j.synthmet.2011.05.011

Razak, S. I. A., Wahman, W. A. W. A., and Yahya, M. Y. (2013). "Novel epoxy resin composites containing polyaniline coated short kenaf bast fibers and polyaniline nanowires: Mechanical and electrical properties," *Journal of Polymer Engineering*, 33(6), 565-577. DOI: 10.1515/polyeng-2012-0152

Razak, S. I. A., Sharif, N. F. A., and Nayan, N. H. M. (2014). "Electrically conductive paper of polyaniline modified pineapple leaf fiber," *Fibers and Polymers* 15(6), 1107-1111. DOI: 10.1007/s12221-014-1107-x

Rudge, A., Davey, J., Raistrick, I., Gottesfeld, S., and Ferraris, J. P. (1994). "Conducting polymers as active materials in electrochemical capacitors," *J. Power Sources* 47(2), 89-107. DOI: 10.1016/0378-7753(94)80053-7

Sainz, R., Benito, A. M., Martínez, M. T., Galindo, J. F., Sotres, J., Baró, A. M., Corraze, B., Chauvet, O., Dalton, A. B., and Baughman, R. H. (2005). "A soluble and highly functional polyaniline–carbon nanotube composite," *Nanotechnology*, 16(5), 150–S154. DOI: 10.1088/0957-4484/16/5/003

Šeděnková, I., Trchová, M., and Stejskal, J. (2008). "Thermal degradation of polyaniline films prepared in solutions of strong and weak acids and in water – FTIR and Raman spectroscopic studies," *Polym. Degrad. Stab.* 93(12), 2147-2157. DOI: 10.1016/j.polymdegradstab.2008.08.007

Segal, A.W., and Meshulam, T. (1979). "Production of superoxide by neutrophils: A reappraisal," *FEBS. Lett.* 100(1), 27-32. DOI: 10.1016/0014-5793(79)81124-2

Sehaqui, H., Zhou, Q., Ikkala, O., and Berglund, L.A. (2011). "Strong and tough cellulose nanopaper with high specific surface area and porosity," *Biomacromolecules* 12(10), 3638–3644. DOI: 10.1021/bm2008907

Shi, X., Zhang, L., Cai, J., Cheng, G., Zhang, H., Li, J., and Wang, H. (2011). "A facile construction of supramolecular complex from polyaniline and cellulose in aqueous system," *Macromolecules*, 44(12), 4565-4578. DOI: 10.1021/ma2009904

Shi, Z., Zang, S., Jiang, F., Huang, L., Lu, D., Ma, Y., and Yang, G. (2012). "In-situ nano-assembly of bacterial cellulose–polyaniline composites," *RSC. Adv.* 2(3), 1040–1046. DOI: 10.1039/C1RA00719J

Stejskal, J., Kratochvíl, P., and Helmstedt, M. (1996). "Polyaniline dispersions poly(vinyl alcohol) and poly(N-vinylpyrrolidone) as steric stabilizers," *Langmuir* 12(14), 3389-92. DOI: 10.1021/la9506483

Vandenberg, O., Schroeter, M., Capadona, J. R., and Weder, C. (2007). "Nanocomposites based on cellulose whiskers and (semi)conducting conjugated polymers," *J. Mater. Chem.* 12 (17), 2746-2753. DOI: 10.1039/b700878c

Wang, X., Wang, X., Wu, Y., Bao, L., and Wang, H. (2010). "Interfacial synthesis of polyaniline nanostructures induced by 5-sulfosalicylic acid," *Mater. Lett.* 64(17), 1865-1867. DOI: 10.1016/j.matlet.2010.06.006

Yu, H., Wang, C., Zhang, J., Li, H., Liu, S., Ran, Y., and Xia, H. (2012). "Cyclodextrin-assisted synthesis of water-dispersible polyaniline nanofibers by controlling secondary growth," *Mater. Chem. Phys.* 133(1), 459-464. DOI: 10.1016/ j.matchemphys. 2012.01.065

Zhang, L., and Wan, M. (2003). "Self-assembly of polyaniline-from nanotubes to hollow microspheres," *Adv. Funct. Mater.* 13, 815-820. DOI: 10.1002/adfm.200304458

Zhang, X., Zhu, J., Haldolaarachchige, N., Ryu, J., Young, D. P., Wei, S., and Guo, Z. (2012). "Synthetic process engineered polyaniline nanostructures with tunable morphology and physical properties," *Polymer* 53(10), 2109-2120.

Article submitted: January 10, 2016; Peer review completed: March 17, 2016; Revised version received and accepted: August 1, 2016; Published: August 24, 2016.
DOI: 10.15376/biores.11.4.8535-8547